CRITERION FOR THREE-FLUID CONFIGURATIONS INCLUDING LAYERS IN A PORE WITH NON-UNIFORM WETTABILITY

MARINUS I.J. VAN DIJKE[1], MOHAMMAD PIRI[2], KENNETH S. SORBIE[1] AND MARTIN J. BLUNT[3]

[1] *Institute of Petroleum Engineering, Heriot-Watt University, Edinburgh EH14 4AS, UK*

[2] *Department of Chemical and Petroleum Engineering, University of Wyoming, Laramie, WY 82071-2000, USA*

[3] *Department of Earth Science and Engineering, Imperial College, London SW7 2AZ, UK*

ABSTRACT

Recently, a considerable effort has been made to determine the precise displacement criteria for three-fluid configurations in pores of angular cross-sections. These configurations may contain thick conducting fluid layers, such as oil layers residing between gas in the centre and water in the corners of the pore. For pores of uniform, but arbitrary, wettability and in the absence of contact angle hysteresis, a precise thermodynamic criterion for the existence of such layers has been established. In this paper we derive similar criteria for layers in pores of non-uniform wettability, where additional and more complicated layer configurations arise. The criteria for formation and removal of layers are consistent with the capillary entry conditions for the accompanying three-phase bulk displacements, which is essential for the accurate pore-scale modelling of three-phase flow. We consider the particular case of three-phase gas invasion in a star-shaped pore with a specific choice of interfacial tensions and contact angles. For this case all possible fluid configurations arise, but only if the water-wet surface in the pore corners is small.

1. INTRODUCTION

Pore-scale network modelling of multi-phase flow, say water, oil (NAPL) and gas (air), crucially depends on the entry conditions for displacement events in individual pores. For two-phase flow in pores with non-circular cross-section, entry pressures for bulk displacements, in the presence of wetting films, can be calculated using the Mayer, Stowe and Princen (MS-P) MS-P theory [e.g. *Lago and Araujo* [2001]. *Van Dijke and Sorbie* [2003] have extended this theory, which is based on minimisation of the free energy, to three-phase capillary entry pressures. Additionally, in three-phase flow layers may form, sandwiched between the bulk phase in the pore centre and the wetting phase in the pore corner, which may significantly enhance the layer phase relative permeability. *Van Dijke et al.* [2004] have shown that the phase pressure combinations associated with displacements of these layers can also be calculated using the above theory. As a result, for a pore of given shape and (uniform) arbitrary wettability, the space of three-phase pressure combinations is uniquely delineated with respect to the possible pore cross-sectional fluid occupancies, where the separations are

given by the entry conditions related to either bulk or layer displacements [*van Dijke and Sorbie,* 2006b]. Using a capillary bundle model, *van Dijke and Sorbie* [2006b] showed that implementation of these criteria may have a major effect on the simulation of three-phase displacements processes, such as NAPL migration in the unsaturated zone and gas injection for improved oil recovery.

A further complication arises in pores, which have undergone a wettability change after primary drainage [*Kovscek et al.*, 1993]. Combining the MS-P theory for two-phase displacements in these so-called Kovscek pores [*Ma et al.*, 1996; *Blunt* 1997], and the three-phase capillary entry pressures in uniformly wetted pores [*van Dijke and Sorbie*, 2003; *van Dijke et al.*, 2004], *Piri and Blunt* [2004] and *Helland and Skjaeveland* [2006] calculated two-phase and three-phase capillary entry pressures for piston-like displacements in Kovscek pores. The stability of layers arising during these displacements was assessed using a geometrical layer collapse criterion [*Hui and Blunt*, 2000]. As a preliminary to this paper, *van Dijke and Sorbie* [2006a] recently derived the thermodynamic criteria for displacements involving an oil layer sandwiched between water in the centre and in the corners of a Kovscek pore during a two-phase water flood.

The main purpose of this paper is to derive the proper three-phase flow thermodynamic criteria for the existence of fluid layers in a Kovscek pore and to demonstrate how these fit in with the capillary entry pressures for the corresponding bulk displacements. Rather than deriving an abstract general theory, we choose a specific range of contact angles and the related phase wetting order, as well as a specific pore geometry, and discuss the arising fluid configurations and displacements with their entry conditions. This case is general enough to be extended straightforwardly to other cases or we make comments to this end.

2. MODEL

2.1 Displacement scenarios and pore fluid configurations

As a model pore, we consider a straight tube with a cross-section shaped as a regular three-cornered star, with corner half angle $\gamma \leq \pi/6$, as shown in Figure 1. After primary drainage (oil invasion into the water-filled water-wet pore) the surface in the centre of the pore, which was contacted by oil, has become more oil-wet than the corners of the pore, where water remains. As an example, Figure 1 shows the possible situation after an increase of the water pressure, followed by gas invasion. The latter has displaced most of the oil in the centre, leaving oil layers behind. Below, we describe the possible displacement scenarios during gas invasion into the different pore fluid occupancies resulting from a water flood following primary drainage.

The maximum oil-water pressure difference P_{ow}^{dr} reached at the end of the primary drainage process determines the length of contact L_s^{dr} (between water and solid) of the corner surface that does not change wettability. Drainage has taken place at a contact angle θ_{ow}^{dr} (taken as 0). P_{ow}^{dr} is usually larger than the MS-P oil-water capillary entry pressure P_{ow}^{MSP}. For processes following drainage, we define at the water-wet (unaltered) surface receding and advancing oil-water contact angles $\theta_{ow,r}^{w}$ and $\theta_{ow,a}^{w}$. On the oil-wet (altered) surface in the centre of the pore we define $\theta_{ow,r}^{o}$ and $\theta_{ow,a}^{o}$.

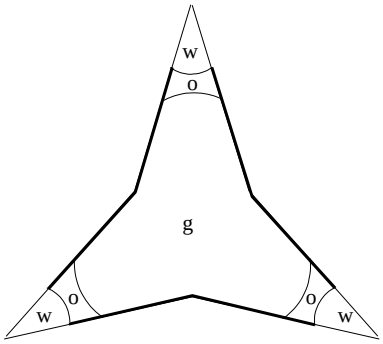

FIGURE 1. Cross-section of a star-shaped pore with water wetting layers in the corners, gas in the centre and oil layers in between. Bold lines indicate surfaces of altered wettability.

A water flood following primary drainage may lead to pore fluid occupancies B, D or A, sketched in Figure 2 for an equilateral triangle (a star with $\gamma = \pi/6$), for subsequently larger water pressures respectively. More precisely, water invasion in configuration B may either lead directly to configuration A (B→A) and the entry condition for the corresponding bulk displacement is given by *Ma et al.* [1996] or a bulk displacement from B to D followed by a layer displacement from D to A may occur (B→D→A) [*Piri and Blunt*, 2004; *van Dijke and Sorbie* 2006a]. The relevant contact angles during water invasion are $\theta^w_{ow,a}$ and $\theta^o_{ow,a}$, where the (outer) oil-water arc meniscus (ow AM) in the corners is pinned at the contact length L_s^{dr} with the hinging angle $\theta_{ow,h}$ satisfying $\theta^w_{ow,a} < \theta_{ow,h} < \theta^o_{ow,a}$. We assume that $\theta^o_{ow,a}$ is large enough to prevent configurations B and D with the outer AM in a stable position on the oil-wet surface. In fact, presence of the inner AM in configuration D requires $\theta^o_{ow,a} > \pi/2 + \gamma$.

Gas invasion into configurations A, B and D may then lead to the remaining configurations sketched in Figure 2 as part of the series of displacements indicated below, if we assume that gas is wetting to water on the oil-wet surface, i.e. the gas-water contact angles $\theta^o_{gw,r}$ and $\theta^o_{gw,a}$ are larger than $\pi/2$. During gas invasion the relevant gas-water angles are the receding angles $\theta^w_{gw,r}$ and $\theta^o_{gw,r}$, for which we assume $\theta^o_{gw,r} > \pi/2 + \gamma$ and $\theta^w_{gw,r} < \theta^o_{gw,r}$. The former condition allows presence of the (inner) gw AM on the oil-wet surface, for example in configuration E. The latter condition may cause the outer gw AM to be pinned with hinging angle $\theta_{gw,h}$ satisfying $\theta^w_{gw,a} < \theta_{gw,h} < \theta^o_{gw,a}$. Similarly, we use receding gas-oil contact angles $\theta^w_{go,r}$ and $\theta^o_{go,r}$ with $\theta^o_{go,r} < \pi/2 - \gamma$, to allow the presence of the go AM on the oil-wet surface and $\theta^w_{go,r} > \theta^o_{go,r}$. During gas invasion the oil-water contact angles are taken from the preceding water flood.

Gas invasion into configurations A, B or D may involve the following series of displacements "visiting" the indicated configurations:

1.	A→C	4.	B→F →C	7.	D→F→C
2.	A→E →C	5.	D→C	8.	D→G→E→C
3.	B→C	6.	D→E→C	9.	D→G→F→C

all eventually resulting in configuration C if the gas pressure can be increased sufficiently. Obviously, series may terminate earlier if the latter is not the case.

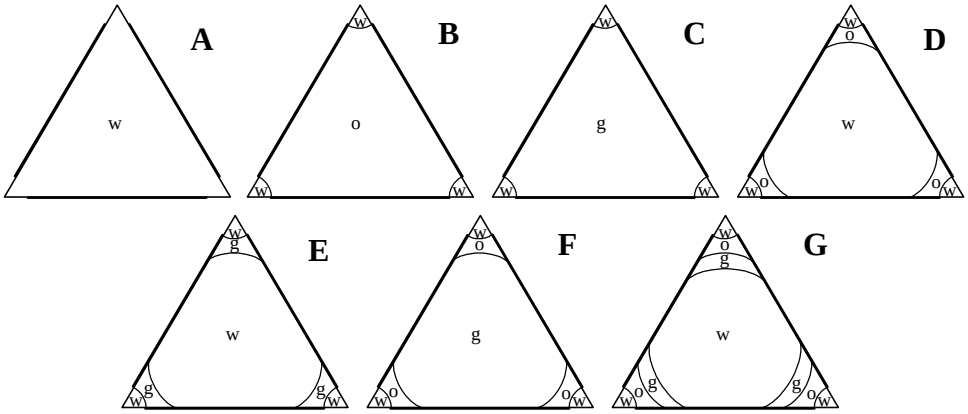

FIGURE 2. Cross-sectional configurations associated with three-phase gas invasion, when gas is wetting to water on the surface of altered wettability.

Displacements A→C, B→C, B→F, D→C, D→F, E→C and G→F involving a change of bulk phase from water (or oil) to gas, have been analysed in detail by *Piri and Blunt* [2004] and *Helland and Skjaeveland* [2006]. However, the remaining displacements D→E, D→G, F→C and G→E involving formation or removal of layers have not been studied, other than based on a geometrical layer collapse criterion or in uniformly wetted pores. Furthermore, although configurations E and G were anticipated before, they could not be produced during gas invasion using bulk displacement and layer collapse mechanisms only.

2.2 Free energy balance

In general, the capillary entry pressures and layer displacement criteria are calculated from minimisation of the free energy differential dF for a small displacement dx of the fluids along the pore, where one cross-sectional configuration displaces another. In Figure 3, a slice along the pore, through one corner is shown for displacement D→E. The cross-sectional configurations meet at the main terminal meniscus (MTM). The general equation for the variation of free energy is [e.g. *Piri and Blunt*, 2004]

$$dF = P_{gw}dV_w + P_{go}dV_o + \sigma_{gw}\left(dA_{gw} - \cos\theta_{gw}^{MTM}\,dA_{ws}\right) + \sigma_{go}\left(dA_{go} - \cos\theta_{go}^{MTM}\,dA_{os}\right) + \sigma_{ow}dA_{ow} \quad (1)$$

where dV_i denotes the change of volume of phase i, dA_{is} denotes the change of the fluid-solid contact area for phases i, and dA_{ij} denotes the change of the fluid-fluid contact area between phases i and j. Furthermore, equation (1) contains the interfacial tensions σ_{ij} and two contact angles at the MTM, where the third possible contact angle θ_{ow}^{MTM} follows from the Bartell-Osterhof equation $\sigma_{gw}\cos\theta_{gw} = \sigma_{go}\cos\theta_{go} - \sigma_{ow}\cos\theta_{ow}$.

The minimum free energy is obtained by solving the equation $dF = 0$ for the radii of curvature r_{ij} ($ij = gw, go, ow$), which are related to the pressure differences as $P_{ij} = \dfrac{\sigma_{ij}}{r_{ij}}$ and related to each other through $P_{gw} = P_{go} + P_{ow}$. Using the latter equation, the solution of equation (1) is a functional relation between two of the radii.

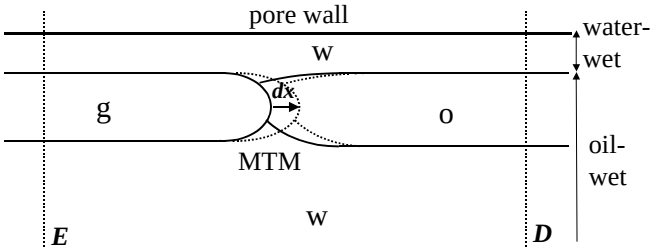

FIGURE 3. Slice along the pore through one of the corners for a small movement dx of the main terminal meniscus (MTM) associated with displacement D→E.

As an example, we give the expressions for the volume and area changes related to the layer displacement D→E, i.e.

$$dV_w = \left\{-3\left(A^{(\alpha)}\left(r_{wg},\theta_{wg}^{AM2}\right)-A^{(\alpha)}\left(r_{wo},\theta_{wo}^{AM2}\right)\right)-3\left(A^{(\alpha)}\left(r_{ow},\theta_{ow}^{AM1}\right)-A^{(\alpha)}\left(r_{gw},\theta_{gw}^{AM1}\right)\right)\right\}dx$$

$$dV_o = -3\left(A^{(\alpha)}\left(r_{wo},\theta_{wo}^{AM2}\right)-A^{(\alpha)}\left(r_{ow},\theta_{ow}^{AM1}\right)\right)dx \qquad (2a)$$

$$dA_{ws} = \left\{-3\left(L_s^{(\alpha)}\left(r_{wg},\theta_{wg}^{AM2}\right)-L_s^{(\alpha)}\left(r_{wo},\theta_{wo}^{AM2}\right)\right)-3\left(L_s^{(\alpha)}\left(r_{ow},\theta_{ow}^{AM1}\right)-L_s^{(\alpha)}\left(r_{gw},\theta_{gw}^{AM1}\right)\right)\right\}dx,$$

$$dA_{os} = -3\left(L_s^{(\alpha)}\left(r_{wo},\theta_{wo}^{AM2}\right)-L_s^{dr}\right)dx \qquad (2b)$$

$$dA_{gw} = 3L_f^{(\alpha)}\left(r_{wg},\theta_{wg}^{AM2}\right)+3L_f^{(\alpha)}\left(r_{gw},\theta_{gw}^{AM1}\right)dx,\ dA_{go}=0,$$

$$dA_{ow} = -3\left(L_f^{(\alpha)}\left(r_{wo},\theta_{wo}^{AM2}\right)+L_f^{(\alpha)}\left(r_{ow},\theta_{ow}^{AM1}\right)\right)dx \qquad (2c)$$

where the geometrical functions $A^{(\alpha)}\left(r_{ij},\theta_{ij}\right)$, $L_s^{(\alpha)}\left(r_{ij},\theta_{ij}\right)$, $L_f^{(\alpha)}\left(r_{ij},\theta_{ij}\right)$ arising in a corner α are explained in the Appendix. The superscripts AM1 and AM2 refer to the outer and inner menisci in the corners respectively. We solve equation (1) for r_{gw} as a function of r_{ow}. Since AM2 arises on the oil-wet surface, $\theta_{wo}^{AM2}=\pi-\theta_{ow,a}^{o}$, which is taken from the preceding water flood and $\theta_{wg}^{AM2}=\pi-\theta_{gw,r}^{o}$.

For this displacement at least the ow AM1 is pinned at the contact length L_s^{dr}, with the hinging angle $\theta_{ow}^{AM1}=\theta_{ow,h}$. Assuming that L_s^{dr} is known from the primary drainage process and r_{ow} from the end of the preceding waterflood, $\theta_{ow,h}$ follows from equation (A.1b), with $L_s^{dr}=L_s^{(\alpha)}\left(r_{ow},\theta_{ow,h}\right)$. Similarly, the gw AM1 may be pinned, but in this case r_{gw} and $\theta_{gw,h}$ are both unknown. Therefore, we take equation (A.1b) as an additional constraint, i.e.

$$L_s^{dr}=2r_{gw}\frac{\cos\left(\theta_{gw,h}+\gamma\right)}{\sin\gamma} \qquad \text{for} \qquad \theta_{gw,r}^{w}<\theta_{gw,h}<\theta_{gw,r}^{o} \qquad (3)$$

However, it is not a priori known that the gw AM1 is actually pinned as it could also be present on the water-wet surface. To resolve this technicality, we calculate the threshold value

r_{gw}^* from $L_s^{dr} = L_s^{(\alpha)}\left(r_{gw}^*, \theta_{gw,r}^w\right)$ at which AM1 is about to enter the water-wet surface. Then, we take $\theta_{gw}^{AM1} = \theta_{gw,r}^w$ if $r_{gw} < r_{gw}^*$ and calculate $\theta_{gw}^{AM1} = \theta_{gw,h}$ from equation (3) if $r_{gw} > r_{gw}^*$.

At the MTM the contact angles in equation (1) are $\theta_{go}^{MTM} = \theta_{go,r}^o$ and $\theta_{gw}^{MTM} = \theta_{gw,r}^o$, although strictly the term $\cos\theta_{gw}^{MTM} dA_{ws}$ should be split in a water-wet and an oil-wet part if AM1 arises on the water-wet surface.

For completeness, we also give the expressions for the volume and area changes related to a bulk displacement, for example for G→F, which involve the total cross-sectional area A and perimeter L_s

$$dV_w = -\left(A - 3A^{(\alpha)}\left(r_{wg}, \theta_{wg}^{AM2}\right)\right)dx,\ dV_o = 0 \tag{4a}$$

$$dA_{ws} = -\left(L_s - 3L_s^{(\alpha)}\left(r_{wg}, \theta_{wg}^{AM2}\right)\right)dx,\ dA_{os} = 0 \tag{4b}$$

$$dA_{gw} = 3L_f^{(\alpha)}\left(r_{wg}, \theta_{wg}^{AM2}\right)dx,\ dA_{go} = 0,\ dA_{ow} = 0 \tag{4c}$$

Notice that these expressions are the same as for a "classical" displacement, as no hinging angles occur, and an analytical solution for r_{gw}, in this case independent of r_{ow}, is available [*van Dijke and Sorbie*, 2003]. Furthermore, the same expressions are found for displacement E→C. Similarly, identical expressions arise for displacements G→E and F→C.

2.3 Computational procedure

For primary drainage an analytical solution of the equation $dF = 0$, for which dF in equation (1) reduces to a simple two-phase expression, is readily available [e.g. *Ma et al.* 1996] to determine the corresponding r_{ow}, hence P_{ow}^{MSP}. For the water flood displacements B→A, B→D and D→A a simple Newton-Raphson method is used to determine the zeros of dF, i.e. values of r_{ow} and the accompanying value of $\theta_{ow,h}$ when relevant, although for B→D also an analytical solution is available [e.g. *van Dijke and Sorbie*, 2006a]. For gas invasion, we calculate for a series of r_{ow} (with $\theta_{ow,h}$) resulting from the water flood, solutions of $dF = 0$, also using a Newton-Raphson method, where equation (3) is used to determine the possible hinging angles.

Since for most displacements two solutions arise, we carefully check if the obtained solutions are physically possible. Usually, one of the two solutions is ruled out as it involves a radius of curvature for one or more of the AMs that is larger than the snap-off value, which is found from equation (A.1b) with $L_s^{(\alpha)} = L_s / 3$. For example, for configuration E the snap-off value for the inner AM1 is found from $L_s^{(\alpha)}\left(r_{gw}, \theta_{gw,r}^o\right)$. Furthermore, for configurations involving layers, we check if the geometrical collapse criteria [*Hui and Blunt*, 2000] have not been violated. These criteria simply state that the AMs surrounding a layer should not touch and can be derive from geometrical expression for the contact lengths as given in the Appendix.

3. RESULTS AND DISCUSSION

We calculate the entry pressures related to all possible displacements in series 1 to 9 for gas invasion using the following parameters: interfacial tensions $\sigma_{gw} = 30$ mN/m, $\sigma_{go} = 10$ mN/m, $\sigma_{ow} = 28$ mN/m; relevant contact angles $\theta^{w}_{ow,a} = 0.760$, $\theta^{o}_{ow,a} = 3.14$, $\theta^{w}_{gw,r} = 0.182$, $\theta^{o}_{gw,r} = 2.22$, $\theta^{w}_{go,r} = 0.400$ and $\theta^{o}_{go,r} = 0.200$. A small corner angle of $\gamma = 0.131$ is used. The entry pressures are determined for three different maximum drainage oil-water pressures relative to the MS-P capillary entry pressure, i.e., $P^{MSP}_{ow} / P^{dr}_{ow} = 0.1$, $P^{MSP}_{ow} / P^{dr}_{ow} = 0.3$ and $P^{MSP}_{ow} / P^{dr}_{ow} = 0.5$, where these ratios are proportional to the contact lengths L^{dr}_{s} of the remaining water-wet surface. In Figure 3 the gas-water pressure differences P_{gw} versus the oil-water pressure differences P_{ow} are presented, where the latter follow from the previous water flood, in case $P^{MSP}_{ow} / P^{dr}_{ow} = 0.1$, showing the different entry pressures. The pressure differences have been normalised through multiplication by r_{in} / σ_{ij} .

Observe first that a number of consistent crossovers occur [*van Dijke and Sorbie*, 2006b], For example the 3 lines corresponding to D→E, D→G and G→E cross in exactly the same point, indicated as (D,G,E). Similarly, crossovers (A,D,C), (A,D,E), (D,F,G), (A,B,C), (B,D,F) and (D,C,F) can be observed, although they are not so easy to see. Remembering that the entry condition for G→E is the same as for F→C and that the entry condition for G→F is the same as for E→C, we find also (C,D,F) and (C,D,E). Finally, using the same identities we find that the crossover of G→E and G→F is actually a special crossover of 4 entry conditions, i.e. (C,E,F,G).

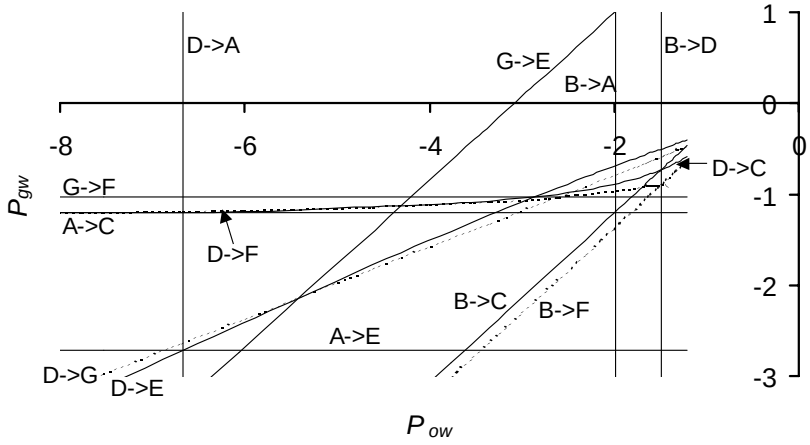

FIGURE 4. Capillary entry pressures and layer displacement criteria in terms of P_{gw} versus P_{ow} for the water flood displacements (vertical lines) and the displacements during the subsequent gas invasion.

Next, we work out which entry pressures and crossovers are actually relevant. The vertical lines represent the water flood entry pressures. A water flood, in which P_{ow} decreases, starting with configuration B at large P_{ow} will first lead to configuration D, at B→D and subsequently to configuration A at D→A making B→A is not relevant.

Gas invasion is represented by increasing P_{gw}, starting from a very small value, at a constant P_{ow}. For example at $P_{ow} = -4$ the two-phase oil water configuration is D, hence during increase of P_{gw} the displacement "away from D" with the lowest entry pressure is D→G. Having arrived at G, the lowest entry pressure "away from G" is G→F. Finally, the lowest entry pressure "away from F" is F→C (i.e G→E). In effect, we have found displacement series 9 for gas invasion. This process of finding the lowest entry pressures can be formalised using the ordering of the free energies for all possible pairs of fluid configurations [*van Dijke and Sorbie*, 2006b].

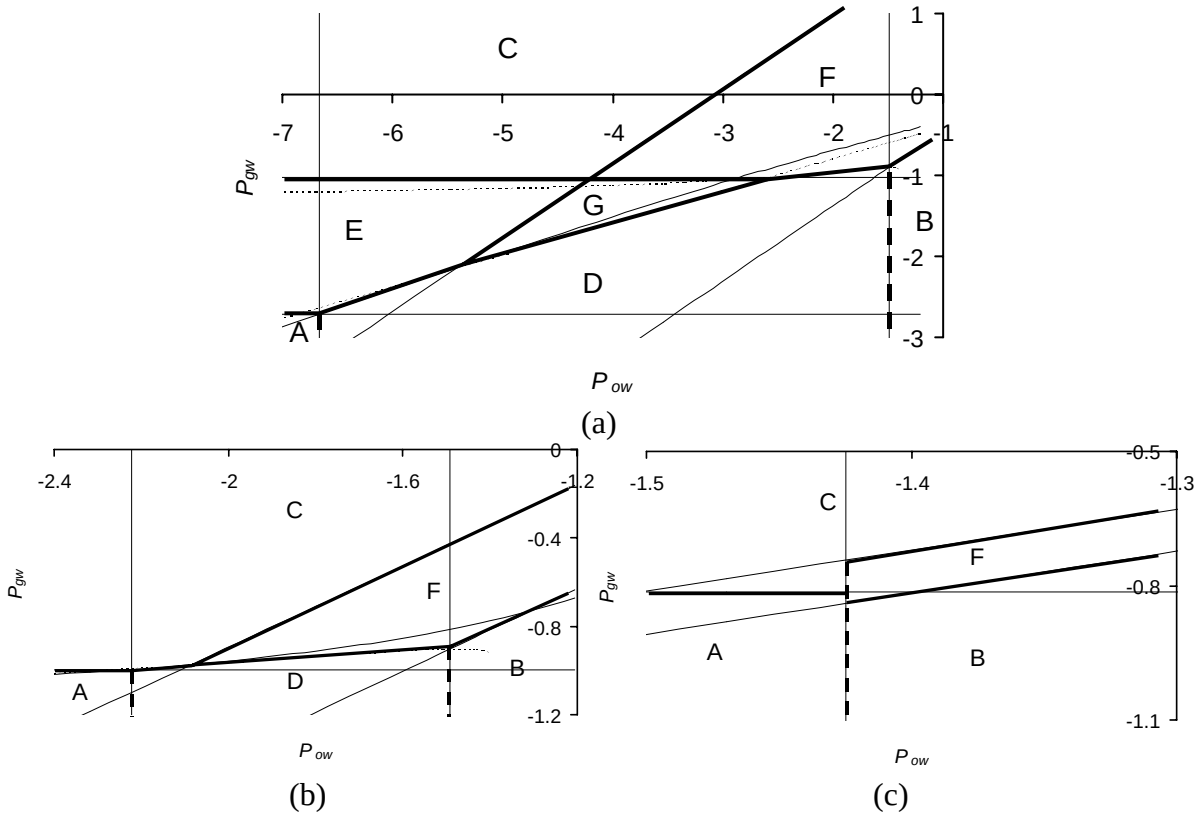

FIGURE 5. Delineation of the $\left(P_{ow}, P_{gw}\right)$ space with respect to the various configurations as presented in Figure 2 using the bold lines for the relevant parts of the displacement criteria for (a) $P_{ow}^{MSP} / P_{ow}^{dr} = 0.1$, (b) $P_{ow}^{MSP} / P_{ow}^{dr} = 0.3$ and (c) $P_{ow}^{MSP} / P_{ow}^{dr} = 0.5$.

After examination of all possible displacement paths between the various crossovers, we present in Figure 5(a) the delineation of the $\left(P_{ow}, P_{gw}\right)$ space with respect to the different configurations of Figure 2. Entry conditions that are not relevant for any pressure combination, such as B→C have been removed. Notice the various remaining relevant crossovers, in particular (C,E,F,G). We conclude that for this high P_{ow}^{dr} (in combination with the small corner half angle) a complicated set of configurations and entry pressures occurs, including configurations E and G, which are formed during the layer displacements D→E and D→G. Additionally, for all the configurations involving layers, related to the relevant entry conditions, we have confirmed that the geometrical collapse criterion is not violated.

In Figure 5(b) the delineation of the $\left(P_{ow}, P_{gw}\right)$ space is presented for $P_{ow}^{MSP}/P_{ow}^{dr} = 0.3$. Although in this situation a range of P_{ow} still arises where configuration D can still occur, the entry pressures for D→E and D→G are now higher than for D→C and D→F, favouring the latter displacements. In Figure 5(c) the delineation of the $\left(P_{ow}, P_{gw}\right)$ space is presented for $P_{ow}^{MSP}/P_{ow}^{dr} = 0.5$. For this relatively low P_{ow}^{dr} the only possible oil-water configurations are A and B, thus further reducing the number of possible configurations.

4. CONCLUSIONS

We have derived the thermodynamic pressure criteria for formation and removal of fluid layers during three-phase flow in an angular pore of non-uniform wettability, embedded in the general theory of deriving three-phase capillary entry pressures for bulk displacements. We have considered the particular case of three-phase gas invasion in a star shaped pore and a particular choice of interfacial tensions and contact angles, which has led to one of the most complicated combinations of pore fluid configurations. Conclusions are:

(i) The pressure criteria for layer displacements are consistent with the entry pressures for bulk displacements. This leads to a unique delineation of the space of pressure combinations with respect to the possible fluid configurations.

(ii) Only for a large drainage pressure, i.e. when the remaining water-wet surface in the pore corners is small, can all possible fluid configurations arise.

Obviously, the full implications of the criteria will become evident after they have been implemented in a pore-scale network model.

APPENDIX: PORE GEOMETRY

For the star-shaped pore cross-section of Figure 1 the cross-sectional area and perimeter are given as $A = \frac{3\sqrt{3}}{2}\frac{\sin\left(\frac{\pi}{3}+\gamma\right)}{\sin\gamma} r_{in}^2$ and $L_s = \frac{3\sqrt{3}}{\sin\gamma} r_{in}$, respectively, where r_{in} is the inscribed radius. The areas and contact lengths in each corner α are defined as

$$A^{(\alpha)} = r^2 \cdot \left(\theta + \gamma^{(\alpha)} - \frac{\pi}{2} + \cos\theta \frac{\cos\left(\theta+\gamma^{(\alpha)}\right)}{\sin\gamma^{(\alpha)}} \right) \tag{A.1a}$$

$$L_s^{(\alpha)} = 2r \frac{\cos\left(\theta+\gamma^{(\alpha)}\right)}{\sin\gamma^{(\alpha)}} \tag{A.1b}$$

$$L_f^{(\alpha)} = 2r \cdot \left(\frac{\pi}{2} - \theta - \gamma^{(\alpha)} \right) \tag{A.1c}$$

with $A^{(\alpha)}\left(r_{ij}, \theta_{ij}\right) = A_{ij}^{(\alpha)}$, $L_s^{(\alpha)}\left(r_{ij}, \theta_{ij}\right) = L_{s,ij}^{(\alpha)}$, $L_f^{(\alpha)}\left(r_{ij}, \theta_{ij}\right) = L_{f,ij}^{(\alpha)}$, which are explained in Figure A.1. Notice that for the regular star $\gamma^{(\alpha)} = \gamma$ is the same for all corners. θ_{ij} is measured

through phase j (second index), while r_{ij} is defined positive when pointing into phase i (first index) and negative when pointing into phase j. Furthermore, $r_{ji} = -r_{ij}$ and $\theta_{ji} = \pi - \theta_{ij}$.

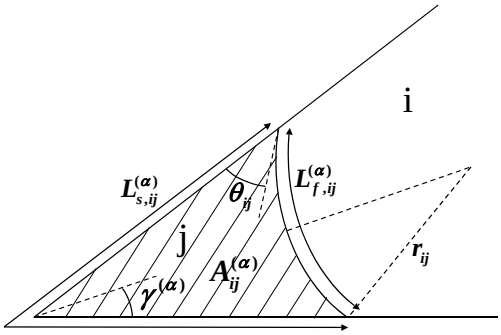

FIGURE A.1 Cross-sectional area $A_{ij}^{(\alpha)}$ occupied by phase j in corner α in the presence of bulk phase i, where the lengths of the surrounding fluid-solid and fluid-fluid contact lines are indicated as $L_{s,ij}^{(\alpha)}$ and $L_{f,ij}^{(\alpha)}$, respectively.

ACKNOWLEDGEMENTS

The authors would like to thank Johan Olav Helland and Svein Skjaeveland for helpful discussions and for a preprint of their paper (SPE99743). M.I.J. van Dijke and K.S. Sorbie acknowledge funding from EPSRC under grant number EP/D002435/1. M. Piri wishes to thank EORI of University of Wyoming for its support.

REFERENCES

Blunt, M.J. (1997), Pore level modeling of the effects of wettability, *SPE J.*, *2*, 494-510.

Helland, J.O. and Skjaeveland, S.M. (2006), Three-phase mixed-wet capillary pressure curves from a bundle-of-triangular-tubes model, *J. Pet. Sci. Eng.*, in press.

Hui, M.-H. and Blunt, M.J. (2000), Effects of wettability on three-phase flow in porous media, *J. Phys. Chem. B*, *104*, 3833-3845.

Kovscek, A.R., Wong, H. and Radke, C.J. (1993), A pore-level scenario for the development of mixed wettability in oil reservoirs, *AIChE J. 39*, 1072-1085.

Lago, M. and Araujo, M. (2001), Threshold pressure in capillaries with polygonal cross section, *J. Colloid Interface Sci.*, *243*, 219-226.

Ma, S., Mason. G. and Morrow., N.R. (1996), Effect of contact angle on drainage and imbibition in regular polygonal tubes, *Colloids and Surfaces*, A. Physicochemical and Engineering Aspects, *117*, 273-291

Piri, M. and Blunt, M.J. (2004), Three-phase threshold capillary pressures in noncircular capillary tubes with different wettabilities including contact angle hysteresis, *Phys. Rev. E.*, *70*, 061603.

van Dijke, M.I.J. and Sorbie, K.S. (2003), Three-phase capillary entry conditions in pores of non-circular cross-section, *J. Colloid Interface Sci.*, *260*, 385-397.

van Dijke, M.I.J., Lago, M, Sorbie, K.S. and Araujo, M. (2004), Free energy balance for three fluid phases in a capillary of arbitrarily shaped cross-section: capillary entry pressures and layers of the intermediate-wetting phase, *J. Colloid Interface Sci.*, *277*, 184-201.

van Dijke, M.I.J. and Sorbie, K.S. (2006a), Existence of fluid layers in the corners of a capillary with non-uniform wettability, *J. Colloid Interface Sci.*, *293*, 455-463.

van Dijke, M.I.J. and Sorbie, K.S. (2006b), Consistency of three-phase capillary entry pressures and pore phase occupancies", *Adv. Water Resour.*, in press.